

See discussions, stats, and author profiles for this publication at: <https://www.researchgate.net/publication/45693850>

# Bis(maltolato)vanadium(III)–Polypyridyl Complexes: Synthesis, Characterization, DNA Cleavage, and Insulin Mimetic Activity

ARTICLE *in* INORGANIC CHEMISTRY · SEPTEMBER 2010

Impact Factor: 4.76 · DOI: 10.1021/ic9025359 · Source: PubMed

CITATIONS

23

READS

75

7 AUTHORS, INCLUDING:



**Avnash Kumbhar**

Savitibai Phule Pune University

28 PUBLICATIONS 412 CITATIONS

SEE PROFILE



**Raymond John Butcher**

Howard University

353 PUBLICATIONS 2,969 CITATIONS

SEE PROFILE



**Menakshi Bhat**

The Ohio State University

12 PUBLICATIONS 206 CITATIONS

SEE PROFILE



**Bimba Joshi**

Agharkar Research Institute

21 PUBLICATIONS 607 CITATIONS

SEE PROFILE

## Bis(maltolato)vanadium(III)-Polypyridyl Complexes: Synthesis, Characterization, DNA Cleavage, and Insulin Mimetic Activity

Md. Nazrul Islam,<sup>†,‡</sup> Anupa A. Kumbhar,<sup>†</sup> Avinash S. Kumbhar,<sup>\*,†</sup> Matthias Zeller,<sup>‡</sup> Raymond J. Butcher,<sup>§</sup> Menakshi Bhat Dusane,<sup>||</sup> and Bimba N. Joshi<sup>||</sup>

<sup>†</sup>Department of Chemistry, University of Pune, Pune-411007, India, <sup>‡</sup>Department of Chemistry, Youngstown State University, Youngstown, Ohio 44555, <sup>§</sup>Department of Chemistry, Howard University, Washington, D.C. 20059, and <sup>||</sup>Institute of Bioinformatics and Biotechnology, University of Pune, Pune-411007, India. <sup>‡</sup>Permanent address: Department of Chemistry, University of Rajshahi, Rajshahi-6205, Bangladesh.

Received December 19, 2009

Four vanadium(III) complexes of the general formula [V(maltol)<sub>2</sub>(N–N)]ClO<sub>4</sub>, where N–N is 2,2′-bipyridine (bpy) (**1**); 1,10-phenanthroline (phen) (**2**); dipyrro[3,2-*d*:2′,3′-*f*]quinoxaline (dpq) (**3**), and dipyrro[3,2-*a*:2′,3′-*c*]phenazine (dppz) (**4**), have been synthesized and characterized by IR, UV–visible, NMR spectroscopies, and electrospray ionization mass spectra (ESI-MS). The complexes exhibit the typical <sup>1</sup>H NMR spectra for paramagnetic V(III) species. The structures of complexes **1**, **2**, and **3** were characterized by single crystal X-ray diffraction. All complexes are monomeric and cationic containing V(III) species ligated to one neutral polypyridyl ligand and two monoanionic bidentate maltolate ligands with a distorted octahedral geometry. The complexes show an irreversible redox peak around +0.80 V versus Ag/AgCl corresponding to one-electron oxidation of V(III) to V(IV). The time-resolved UV–visible spectral changes for the complexes during the electrolysis in acetonitrile solution at +1.0 V are consistent with one-electron oxidation of the complexes to yield the stable V(IV) species. All complexes cleave plasmid pBR322 DNA without the addition of any external agents. In vitro insulin mimetic activity against insulin responsive RIN 5f cells indicates that complex **1** has similar activity to insulin while the others have moderate insulin mimetic activity.

### Introduction

Vanadium coordination chemistry is a topic of interest since the discoveries of it being an essential trace element for certain organisms,<sup>1–4</sup> a cofactor in haloperoxidases<sup>5,6</sup> and nitrogenases,<sup>7,8</sup> and recently as insulin enhancing agents.<sup>9,10</sup> Physiologically relevant oxidation states of vanadium are traditionally thought to be V(IV), as vanadyl, and V(V), often as vanadate.<sup>11</sup> The discovery of the in vivo insulin enhancing

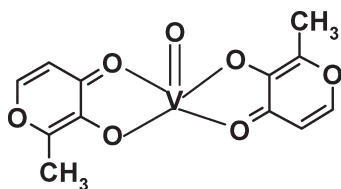
ability of oxovanadium(IV)<sup>9,12–20</sup> and oxovanadate(V)<sup>21–23</sup> complexes and the “benchmark” compound bis(maltolato)oxovanadium(IV),<sup>24</sup> BMOV (Scheme 1) stimulated the search

\*To whom correspondence should be addressed. E-mail: askum@chem.unipune.ac.in. Phone: (+91)-020-25601397 (534). Fax: (+91)-020-25691728.

- (1) *Vanadium in Biological Systems*; Chasteen, N. D., Ed.; Kluwer: Dordrecht, The Netherlands, 1990.
- (2) *Metal Ions in Biological Systems*; Sigel, H., Sigel, A., Eds.; Marcel Dekker, Inc.: New York, 1995; Vol. 31.
- (3) Crans, D. C.; Smee, J. J.; Gaidamauskas, E.; Yang, L. *Chem. Rev.* **2004**, *104*, 849.
- (4) Michibata, H.; Yamaguchi, N.; Uyama, T.; Ueki, T. *Coord. Chem. Rev.* **2003**, *237*, 41.
- (5) Vilter, H. *Phytochemistry* **1984**, *23*, 1387.
- (6) Butler, A.; Walkar, J. V. *Chem. Rev.* **1993**, *93*, 1937.
- (7) Robson, R. L.; Eady, R. R.; Richardson, T. H.; Miller, R. W.; Hawkins, M.; Postgate, J. R. *Nature (London)* **1986**, *322*, 388.
- (8) Eady, R. R. *Coord. Chem. Rev.* **2003**, *237*, 23.
- (9) Thompson, K. H.; McNeill, J. H.; Orvig, C. *Chem. Rev.* **1999**, *99*, 2561.
- (10) Thompson, K. H.; Orvig, C. *Coord. Chem. Rev.* **2001**, *219–221*, 1033.
- (11) Rehder, D. *Angew. Chem., Int. Ed. Engl.* **1991**, *30*, 148.

- (12) Cam, M. C.; Cros, G. H.; Serrano, J. -J.; Lazaro, R.; McNeill, J. H. *Diabetes Res. Clin. Pract.* **1993**, *20*, 111.
- (13) McNeill, J. H.; Yuen, V. G.; Hoveyda, H. R.; Orvig, C. *J. Med. Chem.* **1992**, *35*, 489.
- (14) Sakurai, H.; Fujii, K.; Watanabe, H.; Tamura, H. *Biochem. Biophys. Res. Commun.* **1995**, *214*, 1095.
- (15) Melchior, M.; Thompson, K. H.; Jong, J. M.; Retting, S. J.; Shuter, E.; Yuen, V.; Zhou, Y.; McNeill, J. H.; Orvig, C. *Inorg. Chem.* **1999**, *38*, 2288.
- (16) Watanabe, H.; Nakai, M.; Komazawa, K.; Sakurai, H. *J. Med. Chem.* **1994**, *37*, 876.
- (17) Sakurai, H.; Tsuchiya, K.; Nukatsuka, M.; Kawada, J.; Ishikawa, S.; Yoshida, H.; Komatsu, M. *J. Clin. Biochem. Nutr.* **1990**, *8*, 193.
- (18) Woo, L.; Yuen, V. G.; Thompson, K. H.; McNeill, J. H.; Orvig, C. *J. Bioinorg. Chem.* **1999**, *76*, 251.
- (19) Li, J.; Elberg, G.; Crans, D. C.; Shechter, Y. *Biochemistry* **1996**, *35*, 8314.
- (20) Reul, B. A.; Amin, S. S.; Buchet, J. -P.; Ongemba, L. N.; Crans, D. C.; Brichard, S. M. *Br. J. Pharmacol.* **1999**, *126*, 467.
- (21) Buglyo, P.; Crans, D. C.; Nagy, E. M.; Lindo, R. L.; Yang, L.; Smee, J. J.; Jin, W.; Chi, L.; Godzala, M. E., III; Willsky, G. R. *Inorg. Chem.* **2005**, *44*, 5416.
- (22) Kanamori, K.; Nishida, K.; Miyata, N.; Okamoto, K.; Miyoshi, Y.; Tamura, A.; Sakurai, H. *J. Inorg. Biochem.* **2001**, *86*, 649.
- (23) Song, B.; Aebischer, N.; Orvig, C. *Inorg. Chem.* **2002**, *41*, 1357.
- (24) Melchior, M.; Rettig, S. J.; Liboiron, B. D.; Thompson, K. H.; Yuen, V. G.; McNeill, J. H.; Orvig, C. *Inorg. Chem.* **2001**, *40*, 4686.

Scheme 1. Bis(maltolato)oxovanadium(IV), BMOV



for potential vanadium compounds for the treatment of type II diabetes. Manipulation of the ligands and the various oxidation states of vanadium in an attempt to enhance the insulin mimetic behavior is a topic of recent interest.

Henze's discovery<sup>25</sup> that certain ascidians or sea-squirts sequester V(III) in their blood cells and recent evidence for a new vanadium(III) accumulator in the fan worm *Pseudopotamilla ocellata*<sup>26</sup> spurred the interest of chemists in the coordination chemistry of V(III). A major drawback was the lack of suitable starting materials that can be handled under normal laboratory conditions and the marked tendency of the trivalent state to undergo oxidation. Nonetheless, V(III) is reported to form a large number of multinuclear complexes with aminopolycarboxylates<sup>27</sup> while mononuclear complexes are restricted to chelating agents such as catecholates,<sup>28</sup> salicylideneiminates,<sup>29,30</sup> 8-hydroxyquinolines,<sup>31</sup> oxalates<sup>32</sup> and aminocarboxylates.<sup>27</sup>

Transition metal complexes are also of current interest because of their potential applications as probes of DNA structure, for DNA-dependent electron transfer and site specific cleavage of nucleic acids with the aim of developing novel therapeutic and diagnostic agents.<sup>33</sup> With regard to DNA cleavage activity, more attention has been focused on the middle to late transition metals than the earlier members of the series. Among the latter, vanadium with its three biologically relevant oxidation states (III, IV, and V) has begun to be recognized as a DNA binding and cleaving agent. The bleomycin–vanadyl(IV) complex<sup>34</sup> and  $[\text{VO}(\text{phen})(\text{H}_2\text{O})]^{2+35}$  both have been reported to induce DNA cleavage activity in the presence of  $\text{H}_2\text{O}_2$ . The diperoxovanadium(V) complexes with 2,2'-bipyridine and 1,10-phenanthroline as ancillary ligands have been shown to cleave DNA on photoirradiation.<sup>36–38</sup>

Recently, Chakravarty and co-workers have reported the photoinduced DNA cleavage activity of oxovanadium(IV) complexes of Schiff bases derived from  $\alpha$ -amino acids and phenanthroline bases in the photodynamic therapy (PDT) window.<sup>39</sup> Cationic  $\mu$ -oxo V(III) dimers of the type  $[\text{V}_2\text{OL}_4\text{Cl}_2]^{2+}$  ( $\text{L} = 1,10$ -phenanthroline, 3,4,7,8-tetramethyl-1,10-phenanthroline, 4,7-diphenyl-1,10-phenanthroline, and 2,2'-bipyridine) interact with DNA and degrade DNA probably involving oxidative base loss.<sup>40</sup> These complexes are not only more active DNA cleavage agents than the corresponding monomers, but they do so in the absence of any externally added agents such as  $\text{H}_2\text{O}_2$ .

As part of our ongoing program<sup>41</sup> on the interaction of metal polypyridyl complexes with DNA, we herein describe the synthesis, structures, DNA cleavage, and the in vitro insulin mimetic activity of a series of mixed ligand V(III) complexes of the type  $[\text{V}(\text{maltol})_2(\text{N}-\text{N})]\text{ClO}_4$ , where N–N is 2,2'-bipyridine (bpy) (1), 1,10-phenanthroline (phen) (2), dipyrro[3,2-*d*:2',3'-*f*]quinoxaline (dpq) (3), and dipyrro[3,2-*a*:2',3'-*c*]phenazine (dppz) (4) (Scheme 2). The rationale for this work is to study the DNA cleavage and insulin mimetic activity of an ensemble of polypyridyl ligands with varying intercalating ability, unusual oxidation state of vanadium, namely, vanadium(III), and pro-oxidant coligand, maltol and an overall cationic complex, while hitherto complexes studied in this context are either anionic or neutral.

## Experimental Section

**Materials and Methods.** All chemicals and solvents were reagent grade and were used as received without further purification. The ligands dipyrro[3,2-*d*:2',3'-*f*]quinoxaline (dpq)<sup>42</sup> and dipyrro[3,2-*a*:2',3'-*c*]phenazine (dppz)<sup>43</sup> were synthesized according to the reported procedures. Tris(maltolato)vanadium(III),  $\text{V}(\text{maltol})_3$ , was synthesized following the literature method.<sup>24</sup> The polypyridylum perchlorate salts ( $[\text{bpyH}]^+\text{ClO}_4^-$ ,  $[\text{phenH}]^+\text{ClO}_4^-$ ,  $[\text{dpqH}]^+\text{ClO}_4^-$ , and  $[\text{dppzH}]^+\text{ClO}_4^-$ ) were prepared according to the previously reported method<sup>44</sup> using 1:1 stoichiometric molar ratio of the polypyridyl ligands and perchloric acid in ethanol.

**Physical Measurements.** UV–visible absorption measurements were carried out on a Jasco V-630 spectrophotometer.  $^1\text{H}$  NMR spectra were recorded on a Varian Mercury 300 MHz spectrometer and infrared spectra were obtained on a Shimadzu FTIR-8400 on samples as KBr pellets. Cyclic voltammetric

(25) Henze, M. *Hoppe–Seyler's Z. Physiol. Chem.* **1911**, 7, 494.

(26) Ishii, T.; Nakai, I.; Numako, C.; Okoshi, K.; Otake, T. *Naturwissenschaften* **1993**, 80, 268.

(27) Kanamori, K. *Coord. Chem. Rev.* **2003**, 237, 147.

(28) Cooper, S. R.; Koh, Y. B.; Raymond, K. N. *J. Am. Chem. Soc.* **1982**, 104, 5092.

(29) Bonadies, J. A.; Butler, W. M.; Pecoraro, V. L.; Carrano, C. J. *Inorg. Chem.* **1987**, 26, 1218.

(30) Choudhary, N.; Hughes, D. L.; Klienkes, U.; Larkworthy, L. F.; Leigh, G. J.; Maiwald, M.; Marmion, C. J.; Sanders, J. R.; Smith, G. W.; Sudbrake, C. *Polyhedron* **1997**, 16, 1517.

(31) Manos, M. J.; Tasiopoulos, A. J.; Raptopoulou, C.; Terzis, A.; Woollins, J. D.; Slawin, A. M. Z.; Keramidis, A. D.; Kanabos, T. A. *J. Chem. Soc., Dalton Trans.* **2001**, 1556.

(32) Kittilstved, K. R.; Sorgho, L. A.; Amstutz, N.; Tregenna-Piggott, P. L. W.; Hauser, A. *Inorg. Chem.* **2009**, 48, 7750.

(33) Erkkila, K. E.; Odom, D. T.; Barton, J. K. *Chem. Rev.* **1999**, 99, 2777, and references therein.

(34) Kuwahara, J.; Suzuki, T.; Sugiura, Y. *Biochem. Biophys. Res. Commun.* **1985**, 129, 368.

(35) Sakurai, H.; Tamura, H.; Okatani, K. *Biochem. Biophys. Res. Commun.* **1995**, 206, 133.

(36) Sam, M.; Hwang, J. H.; Chanfreau, G.; Abu-Omar, M. M. *Inorg. Chem.* **2004**, 43, 8447.

(37) Kwong, D. W. J.; Chan, O. Y.; Wong, R. N. S.; Musser, S. M.; Vaca, L.; Chan, S. I. *Inorg. Chem.* **1997**, 36, 1276.

(38) Hiort, C.; Goodisman, J.; Dabrowiak, J. C. *Biochemistry* **1996**, 35, 12354.

(39) Sasmal, P. K.; Patra, A. K.; Nethaji, M.; Chakravarty, A. R. *Inorg. Chem.* **2007**, 46, 11112.

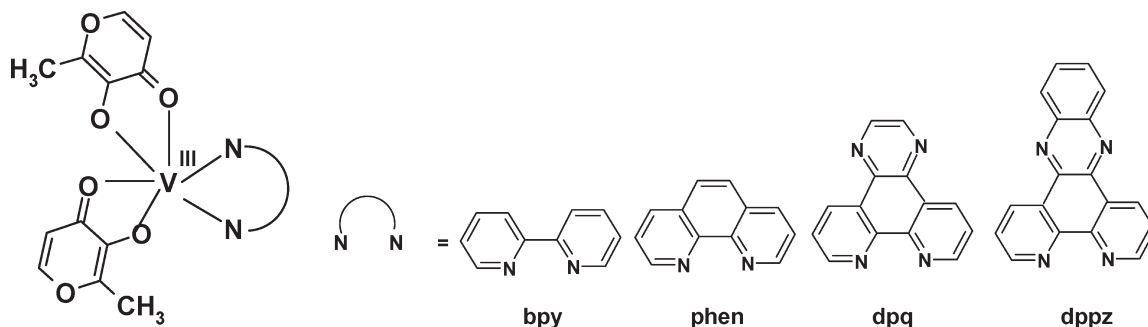
(40) (a) Otieno, T.; Bond, M. R.; Mokry, L. M.; Walter, R. B.; Carrano, C. J. *J. Chem. Soc., Chem. Commun.* **1996**, 37. (b) Heater, S. J.; Carrano, M. W.; Rains, D.; Walter, R. B.; Ji, D.; Yan, Q.; Czernuszewicz, R. S.; Carrano, C. J. *Inorg. Chem.* **2000**, 39, 3881.

(41) (a) Barve, A. C.; Ghosh, S.; Kumbhar, A. A.; Kumbhar, A. S.; Puranik, V. G. *Trans. Met. Chem.* **2005**, 30, 312. (b) Ghosh, S.; Barve, A. C.; Kumbhar, A. A.; Kumbhar, A. S.; Puranik, V. G.; Datar, P. A.; Sonawane, U. B.; Joshi, R. R. *J. Inorg. Biochem.* **2006**, 100, 331. (c) Deshpande, M. S.; Kumbhar, A. A.; Kumbhar, A. S. *Inorg. Chem.* **2007**, 46, 5450. (d) Deshpande, M. S.; Kumbhar, A. A.; Kumbhar, A. S.; Kumbhakar, M.; Pal, H.; Sonawane, U. B.; Joshi, R. R. *Biocjugate Chem.* **2009**, 20, 447. (e) Barve, A.; Kumbhar, A.; Bhat, M.; Joshi, B.; Butcher, R.; Sonawane, U.; Joshi, R. *Inorg. Chem.* **2009**, 48, 9120. (f) Bhat, S. S.; Kumbhar, A. S.; Lönnecke, P.; Hey-Hawkins, E. *Inorg. Chem.* **2010**, 49, 4843. (g) Deshpande, M. S.; Kumbhar, A. S.; Nather, C.; *Dalton Trans.* **2010**, DOI: DT-ART-06-2010-000672.

(42) Collins, J. G.; Sleeman, A. D.; Aldrich-Wright, J. R.; Greguric, I.; Hambley, T. W. *Inorg. Chem.* **1998**, 37, 3133.

(43) Greguric, A.; Greguric, I. D.; Hambley, T. W.; Aldrich-Wright, J. R.; Collins, J. G. *J. Chem. Soc., Dalton Trans.* **2002**, 849.

(44) Kavitha, S. J.; Panchanatheswaran, K.; Elsegood, M. R. J.; Dale, S. H. *Inorg. Chim. Acta* **2006**, 359, 1314.

**Scheme 2.** Mixed Ligand Complexes of V(III) (1–4) and Polypyridyl Ligands Used

measurements were carried out using a set up from CH-1100A instruments, a three-electrode system consisting of platinum as working electrode, platinum-wire as counter electrode, and Ag/AgCl as the reference electrode. Experiments were carried out in acetonitrile solvent containing 0.1 M tetraethylammonium perchlorate (TEAP) as the supporting electrolyte. The total volume utilized was 10–15 mL. The concentrations of the complexes used for oxidation potential measurement were in the range of  $10^{-3}$  M. The spectroelectrochemical behavior of complexes was investigated by controlled potential electrolysis followed by spectral measurement using an Ocean Optics USB 4000 fiber optics spectrophotometer in acetonitrile solution containing 0.1 M TEAP. Electrospray ionization mass spectra (ESI-MS) and high resolution mass spectra (HRMS) of the complexes were recorded on a Q-TOF micromass (YA-105) spectrometer at the Indian Institute of Technology Bombay, Mumbai, India.

**DNA Cleavage Study.** The DNA cleavage experiments were carried out by agarose gel electrophoresis as described earlier.<sup>41</sup> The stock solutions of complexes were prepared in nitrogen saturated dimethylformamide (DMF). Plasmid pBR322 DNA (300 ng) was treated with 300  $\mu$ M samples of the metal complexes, and the mixtures were incubated for 40 min at 37 °C. The reactions after incubation were quenched by the addition of 2  $\mu$ L of gel loading dye (0.25% bromophenol blue, 0.25% xylene cyanol, 40% glycerol, and 2 mM EDTA). The samples were subjected to electrophoresis for 3 h at 60 V on 1% agarose gel in TBE (Tris-Boric acid-EDTA) buffer (pH 8.2). The gel was stained with a 0.5  $\mu$ g/mL ethidium bromide and visualized by UV light and photographed for analysis. The extent of cleavage of the plasmid pBR322 DNA was determined by measuring the intensities of the bands using the Alpha Innotech Gel documentation system (AlphaImager 2200). For mechanistic investigations, experiments were carried out in presence of radical scavenging agents dimethylsulfoxide (DMSO), mannitol, DABCO,  $\text{NaN}_3$ , L-histidine, and SOD which were added to the plasmid pBR322 DNA prior to the addition of the complexes. The concentrations of the complexes, DNA, and the additives corresponding to the final sample volume of 10  $\mu$ L were brought to this volume by addition of deionized water.

**In Vitro Insulin Mimetic Activity.** Insulin responsive cell line RIN 5f was used as the in vitro system to check insulin mimetic activity of the complexes. RIN, clone 5F (RIN 5f), is an *insulinoma cell line* derived from the NEDH rat islet cell tumor from a radiation-induced transplantable rat islet cell tumor.<sup>45</sup> The murine *insulinoma cell line* is an insulin responsive cell line which regulates glucose level in response to insulin. The cell line RIN 5f was cultured in DMEM (Dulbecco's Minimal Essential Medium) containing 10% FBS (Fetal Bovine Serum) and 0.1% antibiotic solution at 37 °C and 5%  $\text{CO}_2$ . The cell line was procured from the National Centre for Cell Sciences, Pune, India.

**In Vitro Glucose Tolerance Test (GTT).** RIN 5f cells were used to check the glucose lowering property of the vanadium complexes. The cells were seeded in 24 well plates at the density of  $10^3$  cells/well. The cells were allowed to adhere overnight at 37 °C and 5%  $\text{CO}_2$ . The DMEM was discarded, and cells were washed with Hank's balanced salt solution (HBSS). The reaction mixtures of 2 mL were prepared by adding HBSS as medium, 500 mM glucose, and complexes with concentration of 1 mM, 500  $\mu$ M, 250  $\mu$ M, and 125  $\mu$ M prepared in DMSO and distilled water. Human recombinant insulin was used as positive control. The supernatant (100  $\mu$ L aliquot) was collected at every 0, 30, 60, 90, 120, and 150 min. The DNSA (dinitrosalicylic acid) assay was used to estimate the glucose concentration. The amount of glucose in the test samples is expressed in millimoles of glucose per 100  $\mu$ L of aliquots collected.

**Glucose Standard Curve.** The glucose standard curve was plotted using 1 mg  $\text{mL}^{-1}$  of stock glucose. The residual glucose in the medium was estimated using the DNSA method, and absorbance was measured at 540 nm.<sup>46,47</sup>

**Synthesis of the Complexes. Caution!** Perchlorate salts of metal complexes with organic ligands are potentially explosive. Although no difficulty was encountered during the synthesis, these should be prepared in small quantities and handled with great care.

**[V(maltol)<sub>2</sub>bpy]ClO<sub>4</sub> (1).** To a solution of V(maltol)<sub>3</sub> (0.166 g, 0.389 mmol) in methanol (20 mL) was added 2,2'-bipyridinium perchlorate, [bpyH]<sup>+</sup>ClO<sub>4</sub><sup>−</sup> (0.100 g, 0.389 mmol). The reaction mixture was refluxed under an atmosphere of nitrogen for 3 h. A brown-red product appeared which was separated by filtration, washed with diethyl ether, and then dried in vacuo. Yield: 0.191 g, 88%. UV-vis (CH<sub>3</sub>CN),  $\lambda_{\text{max}}$ /nm ( $\epsilon/\text{M}^{-1}\text{cm}^{-1}$ ): 216 (50014), 300 (24320), 364 (4692), 456 (1802). IR (KBr,  $\text{cm}^{-1}$ ): 3736 (w), 3614 (w), 3541 (w), 3416 (w), 3068 (w), 1610 (s), 1560 (s), 1471 (s), 1379 (m), 1309 (m), 1269 (s), 1207 (s), 1093 (s), 931 (m), 840 (s), 773 (s), 729 (s), 630 (s), 555 (s), 486 (m), 418 (w). <sup>1</sup>H NMR (DMSO-*d*<sub>6</sub>,  $\delta$ , ppm): −16.4 (br), −11.2 (br), −7.8 (br), −0.5 (br), 7.4 (t), 7.9 (t), 8.3 (d), 11.7 (br), 15.2 (br). ESI-MS (CH<sub>3</sub>CN): *m/z* (%) 457.0 (100) ([M − ClO<sub>4</sub>]<sup>+</sup>), 458.1 (22) ([M − ClO<sub>4</sub> + H]<sup>+</sup>). HRMS: *m/z* calcd for C<sub>22</sub>H<sub>18</sub>N<sub>2</sub>O<sub>6</sub>V ([M − ClO<sub>4</sub>]<sup>+</sup>): 457.0604; found: 457.0618.

Complexes 2–4 were prepared following the procedure described for 1 using [phenH]<sup>+</sup>ClO<sub>4</sub><sup>−</sup>, [dpqH]<sup>+</sup>ClO<sub>4</sub><sup>−</sup>, and [dppzH]<sup>+</sup>ClO<sub>4</sub><sup>−</sup>, respectively, instead of [bpyH]<sup>+</sup>ClO<sub>4</sub><sup>−</sup>.

**[V(maltol)<sub>2</sub>phen]ClO<sub>4</sub> (2).** Yield: 85%. UV-vis (CH<sub>3</sub>CN),  $\lambda_{\text{max}}$ /nm ( $\epsilon/\text{M}^{-1}\text{cm}^{-1}$ ): 220 (63983), 270 (31101), 356 (4976), 464 (1660). IR (KBr,  $\text{cm}^{-1}$ ): 3612 (w), 3435 (w), 3080 (w), 2924 (w), 1612 (s), 1560 (s), 1471 (s), 1379 (w), 1269 (s), 1205 (s), 1097 (s), 929 (m), 848 (s), 773 (w), 727 (s), 628 (s), 555 (m), 486 (m), 430 (w). <sup>1</sup>H NMR (DMSO-*d*<sub>6</sub>,  $\delta$ , ppm): −16.0 (br), −3.9 (br), 6.3 (d), 6.9 (br), 7.7 (m), 7.9 (s), 8.4 (d), 8.7 (s), 9.0 (s), 14.5 (br). ESI-MS (CH<sub>3</sub>CN): *m/z* (%) 481.1 (100) ([M − ClO<sub>4</sub>]<sup>+</sup>), 482.1 (5) ([M − ClO<sub>4</sub> + H]<sup>+</sup>).

(45) Chick, W. L.; Warren, S.; Chute, R. N.; Like, A. A.; Lauris, V.; Kitchen, K. C. *Proc. Natl. Acad. Sci. U.S.A.* **1977**, *74*, 628.

(46) Bhat, M.; Zinjarde, S. S.; Bhargava, S. Y.; Kumar, A. R.; Joshi, B. N. *Evidence-Based Complementary and Altern. Med.* **2008**, *1*.

(47) Miller, G. L. *Anal. Chem.* **1959**, *31*, 426.



Table 1. Crystallographic Data for the Complexes of **1**, **2**, and **3**

	complex <b>1</b>	complex <b>2</b>	complex <b>3</b>
empirical formula	C <sub>22</sub> H <sub>20</sub> ClN <sub>2</sub> O <sub>11</sub> V	C <sub>24</sub> H <sub>18</sub> ClN <sub>2</sub> O <sub>10</sub> V	C <sub>26</sub> H <sub>18</sub> ClN <sub>4</sub> O <sub>10</sub> V
moiety formula	C <sub>22</sub> H <sub>18</sub> N <sub>2</sub> O <sub>6</sub> V, ClO <sub>4</sub> , H <sub>2</sub> O	C <sub>24</sub> H <sub>18</sub> N <sub>2</sub> O <sub>6</sub> V, ClO <sub>4</sub>	C <sub>26</sub> H <sub>18</sub> N <sub>4</sub> O <sub>6</sub> V, ClO <sub>4</sub>
formula weight (g·mol <sup>-1</sup> )	574.79	580.79	632.83
temperature (K)	100	100	100
wavelength (Å)	0.71073	0.71073	0.71073
crystal system	monoclinic	monoclinic	monoclinic
space group	<i>P</i> 2 <sub>1</sub>	<i>P</i> 2 <sub>1</sub> / <i>c</i>	<i>P</i> 2 <sub>1</sub> / <i>n</i>
unit cell dimensions			
<i>a</i> (Å)	7.2047(9)	12.332(4)	17.851(3)
<i>b</i> (Å)	23.247(3)	7.360(2)	8.1865(13)
<i>c</i> (Å)	14.1813(18)	28.958(9)	17.901(3)
$\beta$ (deg)	97.728(2)	91.509(5)	110.51(3)
volume (Å <sup>3</sup> )	2353.6(5)	2627.4(14)	2450.2(7)
<i>Z</i>	4	4	4
density (calcd) (Mg/m <sup>3</sup> )	1.622	1.468	1.715
absorption coefficient (mm <sup>-1</sup> )	0.60	0.54	0.59
<i>F</i> (000)	1176	1184	1288
crystal size (mm <sup>3</sup> )	0.55 × 0.20 × 0.20	0.40 × 0.10 × 0.07	0.33 × 0.13 × 0.05
$\theta$ range for data collection (deg)	2.3–30.6	2.8–25.7	2.4–31.3
index ranges	<i>h</i> = −9→9 <i>k</i> = −27→30 <i>l</i> = −18→18	<i>h</i> = −17→16 <i>k</i> = −10→10 <i>l</i> = −40→40	<i>h</i> = −23→23 <i>k</i> = −10→9 <i>l</i> = −16→23
reflections collected	18759	22291	15394
independent reflections	10757 [ <i>R</i> (int) = 0.027]	7560 [ <i>R</i> (int) = 0.067]	6068 [ <i>R</i> (int) = 0.048]
completeness of $\theta$ = 28.28	28.28°: 99.7%	28°: 98.4%	28.28°: 99.9%
absorption correction	Multiscan Apex2 v2009.7–0 (Bruker, 2009)	Multiscan Apex2 v2009.7–0 (Bruker, 2009)	Multiscan Apex2 v2009.7–0 (Bruker, 2009)
min. and max. transmission	0.746 and 0.665	0.746 and 0.572	0.746 and 0.562
refinement method	full-matrix least-squares on <i>F</i> <sup>2</sup>	full-matrix least-squares on <i>F</i> <sup>2</sup>	full-matrix least-squares on <i>F</i> <sup>2</sup>
data/restraints/parameters	10757/10/712	7560/112/396	6068/0/381
goodness-of-fit on <i>F</i> <sup>2</sup>	1.069	0.951	1.053
final <i>R</i> indices [ <i>I</i> > 2 $\sigma$ ( <i>I</i> )]	<i>R</i> <sub>1</sub> = 0.0553 <i>wR</i> <sub>2</sub> = 0.1362	<i>R</i> <sub>1</sub> = 0.0589 <i>wR</i> <sub>2</sub> = 0.1364	<i>R</i> <sub>1</sub> = 0.0482 <i>wR</i> <sub>2</sub> = 0.1071
<i>R</i> indices (all data)	<i>R</i> <sub>1</sub> = 0.0622 <i>wR</i> <sub>2</sub> = 0.1431	<i>R</i> <sub>1</sub> = 0.1064 <i>wR</i> <sub>2</sub> = 0.1518	<i>R</i> <sub>1</sub> = 0.0779 <i>wR</i> <sub>2</sub> = 0.1214
largest diff. peak and hole (e Å <sup>-3</sup> )	1.61, −0.59	1.14, −0.42	1.33, −0.83

HRMS: *m/z* calcd for C<sub>24</sub>H<sub>18</sub>N<sub>2</sub>O<sub>6</sub>V ([*M* − ClO<sub>4</sub>]<sup>+</sup>): 481.0604; found: 481.0625.

[V(maltol)<sub>2</sub>dppq]ClO<sub>4</sub> (**3**). Yield: 70%. UV–vis (CH<sub>3</sub>CN),  $\lambda_{\text{max}}$ /nm (ε/M<sup>-1</sup> cm<sup>-1</sup>): 217 (69171), 256 (59795), 293 (30128), 464 (2052). IR (KBr, cm<sup>-1</sup>): 3601 (m), 3535 (w) 3080 (m), 1612 (s), 1570 (s), 1473 (s), 1383 (s), 1267 (s), 1205 (s), 1091 (s), 931 (m), 843 (s), 764 (w), 729 (s), 628 (s), 557 (s), 486 (m), 435 (w). <sup>1</sup>H NMR (DMSO-*d*<sub>6</sub>,  $\delta$ , ppm): −16.2 (br), −3.9 (br), −0.5 (br), 1.2 (s), 6.3 (s), 7.9 (s), 8.7 (s), 9.1 (d), 9.3 (s), 10.5 (s), 15.2 (br). ESI-MS (CH<sub>3</sub>CN): *m/z* (%) 533.0 (100) ([*M* − ClO<sub>4</sub>]<sup>+</sup>), 534.0 (14) ([*M* − ClO<sub>4</sub> + H]<sup>+</sup>). HRMS: *m/z* calcd for C<sub>26</sub>H<sub>18</sub>N<sub>4</sub>O<sub>6</sub>V ([*M* − ClO<sub>4</sub>]<sup>+</sup>): 533.0666; found: 533.0676.

[V(maltol)<sub>2</sub>dppz]ClO<sub>4</sub> (**4**). Yield: 93%. UV–vis (CH<sub>3</sub>CN),  $\lambda_{\text{max}}$ /nm (ε/M<sup>-1</sup> cm<sup>-1</sup>): 216 (53506), 276 (54656), 354 (16325), 372 (15459), 464 (2290). IR (KBr, cm<sup>-1</sup>): 3610 (w), 3074 (m), 1612 (s), 1564 (s), 1471 (s), 1415 (m), 1356 (m), 1267 (s), 1205 (s), 1087 (s), 931 (s), 840 (s), 770 (s), 729 (s), 630 (s), 486 (m), 428 (m). <sup>1</sup>H NMR (DMSO-*d*<sub>6</sub>,  $\delta$ , ppm): −16.4 (br), −4.0 (br), 0.8 (br), 1.2 (s), 1.5 (s), 1.9 (s), 5.0 (m) 7.5 to 9.8 (m), 15.5 (br). ESI-MS (CH<sub>3</sub>CN): *m/z* (%) 582.7 (100) ([*M* − ClO<sub>4</sub>]<sup>+</sup>), 583.7 (8) ([*M* − ClO<sub>4</sub> + H]<sup>+</sup>). HRMS: *m/z* calculated for C<sub>30</sub>H<sub>20</sub>N<sub>4</sub>O<sub>6</sub>V ([*M* − ClO<sub>4</sub>]<sup>+</sup>): 583.0822; found: 583.0814.

**X-ray Crystallography.** X-ray quality crystals of the complexes **1**, **2**, and **3** were obtained by solvent diffusion of diethyl ether into a mixture of dimethylformamide and dichloromethane solutions of the complexes. Crystallographic data were collected using a Bruker AXS SMART APEX CCD diffractometer with monochromatic Mo K $\alpha$  radiation (Wavelength  $\lambda$  = 0.71073 Å) with the  $\Omega$  scan technique. Deep red colored crystals were mounted on a Mitegen micromesh mount using a trace of mineral oil and cooled in situ to 100(2) K for data

collection. The data were collected using SMART,<sup>48</sup> and the data integrated and the unit cells determined using SAINT+.<sup>49</sup> The SADABS multiscan absorption correction was applied.<sup>48</sup> The structures were solved by direct methods and refined by full-matrix least-squares against *F*<sup>2</sup> using SHELXTL.<sup>50</sup> A full-matrix least-squares refinement on *F*<sup>2</sup> was used. Nonhydrogen atoms were refined with anisotropic displacement parameters. Carbon bound hydrogen atoms were placed in geometrically idealized positions. For complex **1**, one of the perchlorate ions has three of its oxygen atoms disordered over two mutually exclusive positions with a refined occupancy ratio of 0.55(1) to 0.45(1). Water H atom positions were restrained by hydrogen bonding considerations. In complex **2** large fractions of the unit cell volume are filled with ill defined solvent molecules disordered across a center of inversion for which no satisfactory structural model could be developed. The electron density within these sections was instead corrected for using the Squeeze approach as implemented in Platon<sup>51</sup> (See Squeeze report appended to the cif file). The perchlorate anion is disordered. It was refined as being disordered over three positions with refined occupancy rates of 0.487(2), 0.152(3), and 0.364(5). The Cl–O bonds and the O···O distances were restrained to be all each equal, and strongly overlapping atoms were constrained to have identical anisotropic displacement parameters (O8, O8b and O8c; O7, O7b and O7c; O9 and O9b; Cl1, Cl1b and Cl1c). CCDC 742059, 742060, and 785387 contain the supplementary crystallographic data for **1**, **2**, and **3**, respectively. The data can be obtained free of charge via [www.ccdc.cam.ac.uk/conts/retrieving.html](http://www.ccdc.cam.ac.uk/conts/retrieving.html) (or from

(49) SMART for WNT/2000, version 5.628; Bruker AXS Inc.: Madison, WI, 1997–2002.

(50) SHELXTL, version 6.10; Bruker AXS Inc.: Madison, WI, 2000.

(51) Spek, A. L. *Platon, a Multipurpose Crystallographic Tool*, 40M-Version: 180209; University of Delft: The Netherlands, 2009.

(48) SAINT, version 6.45; Bruker AXS Inc.: Madison, WI, 1997–2003.

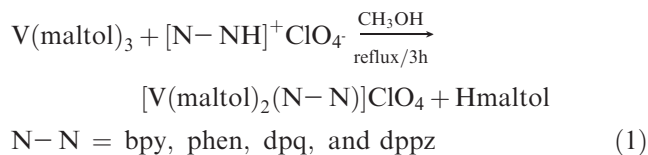
**Table 2.** Selected Bond Lengths [Å] and Angles [deg] for **1**

Bond Lengths [Å]			
V(1)–N(1)	2.139(3)	V(1)–N(2)	2.144(3)
V(1)–O(1)	2.050(3)	V(1)–O(2)	1.915(3)
V(1)–O(4)	2.034(3)	V(1)–O(5)	1.920(3)
N(3)–V(2)	2.140(3)	N(4)–V(2)	2.142(3)
O(7)–V(2)	2.047(3)	O(8)–V(2)	1.923(3)
O(10)–V(2)	1.922(3)	O(11)–V(2)	2.047(3)
Bond Angles [deg]			
O(1)–V(1)–O(4)	172.11(10)	O(1)–V(1)–O(2)	82.22(11)
O(4)–V(1)–O(2)	92.29(11)	O(1)–V(1)–O(5)	93.63(12)
O(4)–V(1)–O(5)	82.33(11)	O(2)–V(1)–O(5)	105.40(12)
O(1)–V(1)–N(2)	93.99(11)	O(4)–V(1)–N(2)	91.68(11)
O(2)–V(1)–N(2)	90.19(13)	O(5)–V(1)–N(2)	163.45(12)
O(1)–V(1)–N(1)	92.73(11)	O(4)–V(1)–N(1)	94.04(11)
O(2)–V(1)–N(1)	163.94(13)	O(5)–V(1)–N(1)	90.08(13)
N(2)–V(1)–N(1)	74.90(13)		
O(10)–V(2)–O(8)	104.15(11)	O(10)–V(2)–O(7)	94.04(11)
O(8)–V(2)–O(7)	82.53(11)	O(10)–V(2)–O(11)	81.90(11)
O(8)–V(2)–O(11)	93.64(12)	O(7)–V(2)–O(11)	173.62(11)
O(10)–V(2)–N(3)	90.96(12)	O(8)–V(2)–N(3)	164.33(12)
O(7)–V(2)–N(3)	92.43(11)	O(11)–V(2)–N(3)	92.56(11)
O(10)–V(2)–N(4)	163.94(13)	O(8)–V(2)–N(4)	91.08(13)
O(7)–V(2)–N(4)	92.94(11)	O(11)–V(2)–N(4)	92.23(12)
N(3)–V(2)–N(4)	74.30(14)		

the Cambridge Crystallographic Data Centre, 12 Union Road, Cambridge CB2 1EZ, U.K.; fax: (+44)1223–336–033; or deposit@ccdc.cam.ac.uk). The crystal structure and refinement data for complex **1**, **2**, and **3** are summarized in Table 1. Selected bond lengths and angles were tabulated in Tables 2 and 3.

## Results and Discussion

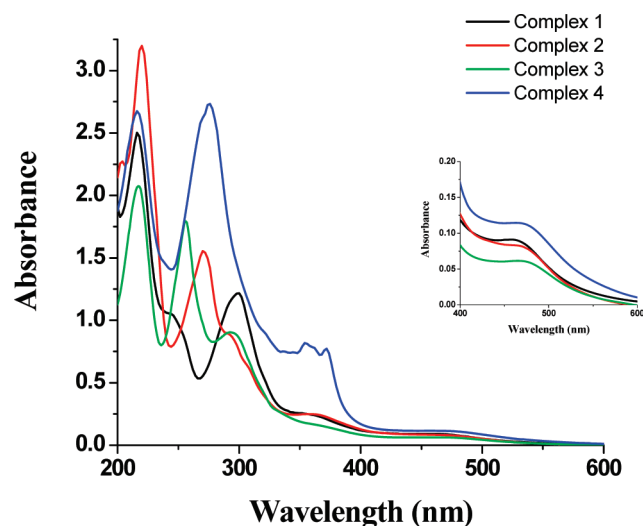
**Synthesis and Characterization.** The complexes were prepared in high yield according to a modified method of Kavitha et al.<sup>44</sup> by treating V(maltol)<sub>3</sub> with protonated polypyridyl perchlorate salts in methanol. The general synthetic method is shown in eq 1. The reaction may be initiated by the dissociation of the polypyridyl salt into free polypyridyl base and acid, followed by the action of acid on V(maltol)<sub>3</sub> to replace one maltolate anion and subsequent coordination of the polypyridyl ligand. As maltolate is a good leaving group, it can thus be replaced by a stronger ligand such as the polypyridyl ligands to obtain the new mixed ligand complexes.



The absorption spectra of the complexes were recorded in acetonitrile solution in the wavelength range of 200–800 nm. There are four transitions observed for complexes **1**–**3**, while five transitions appear for complex **4**. The characteristic bands around 215–300 and 350–380 nm with a molar absorption coefficient in the order of 10<sup>4</sup> M<sup>–1</sup> cm<sup>–1</sup> are assigned to  $\pi\pi^*$  and  $n\pi^*$  transitions respectively. The relatively broad and less intense bands

**Table 3.** Selected Bond Lengths [Å] and Angles [deg] for **2** and **3**

Complex <b>2</b>		Complex <b>3</b>
Bond Lengths [Å]		
V(1)–N(1)	2.147(2)	2.172(2)
V(1)–O(1)	1.918(2)	1.9056(18)
V(1)–O(4)	1.9209(17)	1.9151(18)
V(1)–N(2)	2.154(2)	2.144(2)
V(1)–O(2)	2.0462(18)	2.0423(19)
V(1)–O(5)	2.0404(18)	2.0468(18)
Bond Angles [deg]		
O(1)–V(1)–O(4)	105.79(8)	107.01 (8)
O(4)–V(1)–O(2)	92.69(7)	89.72(8)
O(4)–V(1)–O(5)	82.44(7)	81.79(7)
O(1)–V(1)–N(2)	163.73(8)	162.46(8)
O(2)–V(1)–N(2)	91.70(8)	94.32(8)
O(1)–V(1)–N(1)	89.81(8)	88.16(8)
O(2)–V(1)–N(1)	94.81(7)	91.21(8)
N(2)–V(1)–N(1)	75.61(8)	74.62(8)
O(1)–V(1)–O(2)	82.22(7)	82.49 (7)
O(1)–V(1)–O(5)	94.76(8)	90.91(7)
O(2)–V(1)–O(5)	173.39(7)	167.27(7)
O(4)–V(1)–N(2)	89.49(8)	90.16(8)
O(5)–V(1)–N(2)	92.73(8)	95.16(8)
O(4)–V(1)–N(1)	163.48(8)	164.78(8)
O(5)–V(1)–N(1)	91.05(7)	99.47(8)

**Figure 1.** Electronic spectra of the complexes recorded in CH<sub>3</sub>CN solution. Inset depicts the spectra from 400 to 600 nm.

observed at 464 nm may arise from ligand-orbital ( $p\pi$ ) to metal-orbital ( $p\pi$ ) charge transfers typical of vanadium(III) complexes.<sup>31,52</sup> The electronic spectra of the complexes are shown in Figure 1. The <sup>1</sup>H NMR spectra of the complexes in DMSO-*d*<sub>6</sub> exhibit broadening and shifting of the resonances in the range of +16 to –17 ppm because of the unpaired electron density at the vanadium nuclei. The polypyridyl ligand protons of the complexes display an alternative shift pattern characteristic of contact shift resulting from spin delocalization into the polypyridyl ligands via a  $\pi$ -delocalization pathway.<sup>53,54</sup> As the <sup>1</sup>H NMR signals of mononuclear paramagnetic vanadium(III)

(52) Simpson, C. L.; Pierpont, C. G. *Inorg. Chem.* **1992**, *31*, 4308.

(53) Castro, S. L.; Sun, Z.; Grant, C. M.; Bollinger, J. C.; Hendrickson, D. N.; Christou, G. *J. Am. Chem. Soc.* **1998**, *120*, 2365.

(54) *NMR of Paramagnetic Molecules*; La Mar, G. N., Horrocks, W., De, W., Jr., Holm, R. H., Eds.; Academic Press: New York, 1973.

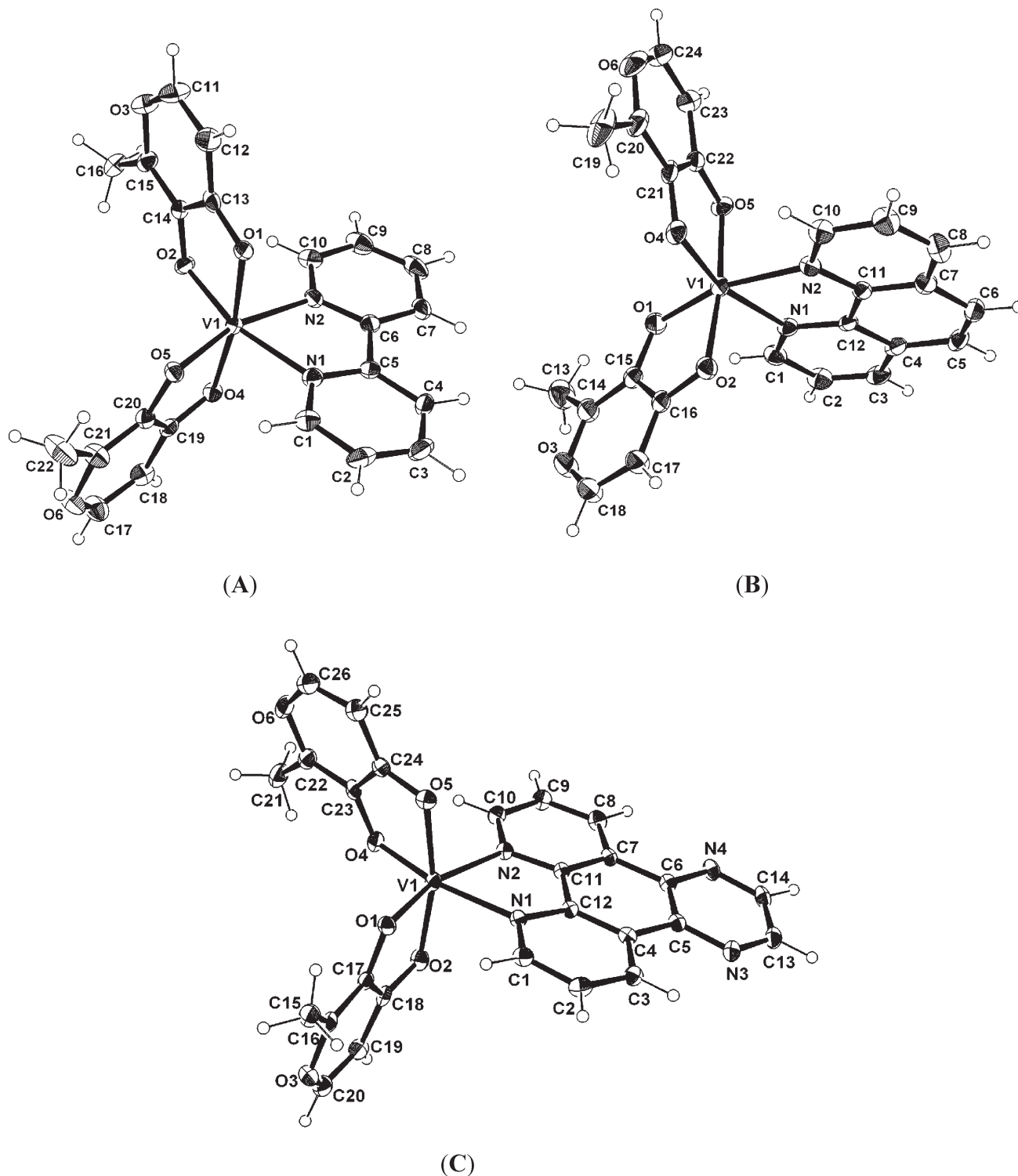


**Figure 2.** ORTEP diagrams of the cationic complexes of (A) **1**, (B) **2**, and (C) **3**. Solvent molecules and perchlorate anions are omitted for clarity (ORTEP plots of the complete structures are provided in the Supporting Information).

complexes are often broadened,<sup>55</sup> the <sup>1</sup>H NMR signals observed in this study are also no exception. The IR frequencies observed between 1470 and 1615 cm<sup>-1</sup> cannot be unambiguously assigned because of the overlapping of pyrone ring vibrations of maltolate ligands with the characteristic ring vibrations of polypyridine ligands. However the frequen-

cies at around 730 ( $\nu_{V-O}$ ) and 418–435 ( $\nu_{V-N}$ ) cm<sup>-1</sup> are indicative of the coordination of maltolate and polypyridyl ligands through their O–O and N–N atoms respectively. The bands observed at around 630 and 1090 cm<sup>-1</sup> are attributed to the ClO<sub>4</sub><sup>-</sup> anion. The positive ion detection mode ESI-MS was used to confirm the compositions of the complexes. The mass spectra of all complexes were dominated by 100% relative intensity ions with *m/z* characteristic of [M – ClO<sub>4</sub>]<sup>+</sup>, and the other

(55) Kumagai, H.; Kitagawa, S.; Maekawa, M.; Kawata, S.; Kiso, H.; Munakata, M. *J. Chem. Soc., Dalton Trans.* **2002**, 2390.

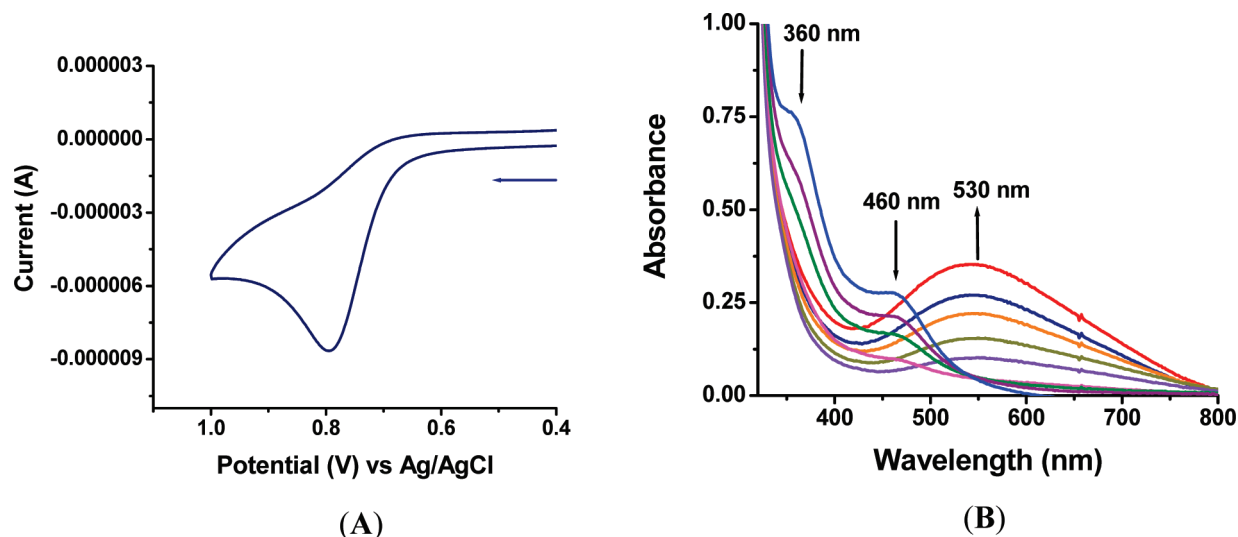


**Figure 3.** (A) Cyclic voltammogram of 1 mM complex **1** at platinum electrode at scan rate of 100 mV s<sup>-1</sup> in CH<sub>3</sub>CN containing 0.1 M TEAP. (B) UV-visible changes during the oxidation of 300 μM complex **1** in acetonitrile containing 0.1 M TEAP.

peaks with less intensity in the spectra were the protonated parent-ion peak corresponding to  $[M - ClO_4 + H]^+$ . The high-resolution MS of the complexes are also in accord with the correct molecular mass and formula. Furthermore, the structures of the complexes **1**, **2**, and **3** have been confirmed by single crystal X-ray diffraction.

**Crystal Structures.** The crystals of complexes **1**, **2**, and **3** were grown by diethyl ether diffusion into a mixture of dimethylformamide and dichloromethane solutions of the complexes. ORTEP representations of the metal cations of **1**, **2**, and **3** with the atom numbering are shown in Figure 2. Full ORTEP plots including the anions and solvate molecules are given in the Supporting Information, Figures S1 to S3. Complex **1** crystallized with two crystallographically independent cations, two perchlorate anions, and two water molecules per asymmetric unit. One of the perchlorate ions has three of its oxygen atoms disordered over two mutually exclusive positions with an occupancy ratio of 0.55(1) to 0.45(1). In complex **2** large fractions of the unit cell volume (326 Å<sup>3</sup>) are filled with ill defined solvent molecules disordered across a center of inversion for which no satisfactory structural model could be developed. The electron density within these sections was instead corrected for using the Squeeze approach as implemented in Platon<sup>51</sup> yielding 106 electrons of disordered solvate molecules that were corrected for. The perchlorate anion in **2** was also disordered with occupancy rates of 0.487(2), 0.152(3), and 0.364(5). The cations in all three compounds show no signs of disorder.

Selected bond lengths and bond angles for **1**, **2**, and **3** are summarized in Table 2–3. In all three compounds the vanadium(III) atoms are in a distorted octahedral coordination geometry formed by two maltolates and one polypyridyl ligand. The ligands coordinate to the vanadium atoms forming five member chelate rings. The vanadium to hydroxido oxygens bond lengths (1.9056–1.9209 Å) in the maltolate ligands are slightly shorter than those to the carboxido oxygens (2.034–2.050 Å); however, the latter bond lengths are well within the range of those in V(III) pyridinonates<sup>24</sup> and catecholates.<sup>28</sup> The distances of vanadium to nitrogen (2.139–2.172 Å) of the polypyridyl

ligands (bpy, phen, dpq) are also in their usual range.<sup>31,56</sup> As the N–V–N bite angles (~75.04°) are smaller than the O–V–O bite angles (~82.24°), the substitution of the maltolate ligand by the polypyridyl ligands (bpy, phen, dpq) causes less steric strain, thus yielding more stable complexes than the precursor complex, V(maltol)<sub>3</sub>. The packing diagrams of complex **1** and **2** show the presence of  $\pi$ – $\pi$  stacking interactions between bpy and phen ligands of neighboring molecules (Supporting Information, Figures S1 and S2), while complex **3** shows  $\pi$ – $\pi$  stacking interaction between maltolate ligands of adjacent molecules (Supporting Information, Figure S3).

**Cyclic Voltammetry and Spectroelectrochemistry.** The cyclic voltammograms of the complexes in acetonitrile with TEAP as supporting electrolyte recorded at room temperature in the potential window of +1.2 to +0.5 V show an irreversible peak around +0.80 V versus Ag/AgCl corresponding to a one electron oxidation of V(III) to V(IV). No peak in the range of +0.0 to +1.2 V has been observed when a blank experiment was carried out with the ligands only. The peak potentials for the V(III)/V(IV) pair are much higher than usually observed for V(III) complexes,<sup>57,58</sup> thus indicating that the complexes are quite stable toward oxidation. A representative CV of complex **1** is shown in Figure 3A.

The spectroelectrochemical behavior of the complexes was investigated using an in situ spectroelectrochemical setup. For the oxidation of the complexes, a constant potential +1.0 V was applied and spectra were recorded during electrolysis. The time-resolved UV-visible spectral changes for complex **1** during the electrolysis in acetonitrile solution containing 0.1 M TEAP is shown in Figure 3B. The initially observed peak at around 460 nm gradually disappears with the concomitant appearance of new peak at 530 nm which is typical of V(IV) species.

(56) Kavitha, S. J.; Panchanatheswaran, K.; Low, J. N.; Glidewell, C. *Acta Crystallogr.* **2006**, E62, 529.

(57) Chatterjee, M.; Ghosh, S.; Nandi, A. K. *Polyhedron* **1997**, 16, 2917.

(58) Chatterjee, M.; Maji, M.; Ghosh, S.; Mak, T. C. W. *J. Chem. Soc., Dalton Trans.* **1998**, 3611.



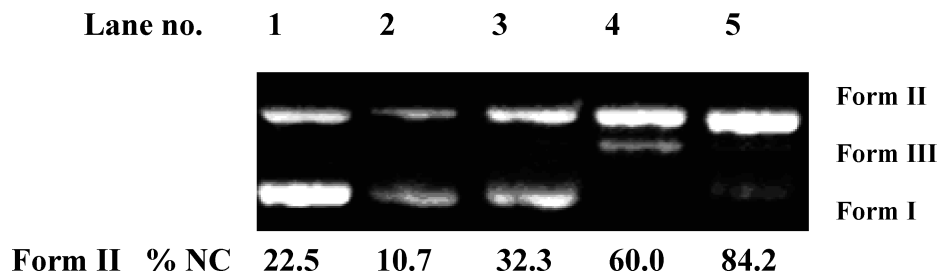


**Figure 4.** Ethidium bromide-stained agarose gel (1%) of 300 ng plasmid pBR322 DNA in the presence of 300  $\mu$ M complexes in  $N_2$  atmosphere. Incubation time: 40 min, 37  $^{\circ}$ C. Lane 1: DNA control, lane 2: DNA + 1, lane 3: DNA + 2, lane 4: DNA + 3, lane 5: DNA + 4.

These changes are consistent with a one-electron oxidation of the complexes to yield the stable V(IV) species.

**DNA Cleavage Studies.** All the reported V(III) complexes 1–4 are sensitive to aerial oxidation in solution, although they are quite stable in the solid state over a period of 2–3 months when kept in a vacuum desiccator. It is known that DNA cleavage is controlled by relaxation of supercoiled circular conformation of pBR322 DNA to nicked circular and/or linear conformations. When electrophoresis is applied to circular plasmid DNA, the fastest migration will be observed for DNA of closed circular conformation (Form I). If one strand is cleaved, the super coil will relax to produce a slower moving nicked conformation (Form II). If both strands are cleaved, a linear conformation (Form III) will be generated that migrates in between. To assess the DNA cleavage ability of the V(III) complexes, plasmid pBR322 DNA (300 ng) was incubated with 300  $\mu$ M of complexes 1–4 in TBE (Tris-Boric acid-EDTA) buffer (pH 8.2) for 40 min at 37  $^{\circ}$ C. It was observed that complexes 1 and 2 show little cleavage ability as compared to 3 and 4 (Figure 4). Further, rapid air oxidation of complexes 1 and 2 rendered the solutions difficult to work with. Therefore, all further studies concentrated on complexes 3 and 4.

Figure 5 indicates the relative amounts of supercoiled (SC) and nicked circular (NC) DNA as a function of concentration of complex 3. More than 80% conversion of SC to NC was observed at 300  $\mu$ M concentration when incubated for 40 min. Additional experiments indicated that the reaction was completed within 20 min at 300  $\mu$ M concentration.

During longer incubation times at low concentrations, the orange color of the complexes faded as the V(III) probably undergoes oxidation to V(IV) as shown by time-resolved UV–visible spectral changes (Figure 3). Similar observations were made by Carrano et al.<sup>40</sup> wherein dimeric V(III) complexes are oxidized to V(IV) monomers with concomitant change in the color from deep violet of the dimer to the pale yellow of the monomer. It is interesting to note that these complexes cleaved DNA in absence of any external reagents like ascorbate or hydrogen peroxide which are usually required for the activation of complexes. It should be noted that though the anaerobic conditions employed were sufficient to prevent any oxidation of V(III) to V(IV), the presence of small amounts of oxygen under the experimental conditions cannot be ruled out.

To investigate the role of radicals in the DNA cleavage by the complexes, reactions were performed in nitrogen atmosphere by incubating the complexes 3 and 4 with

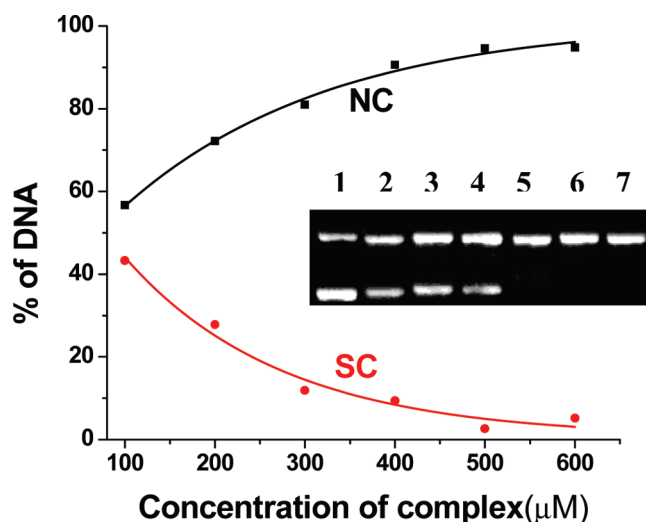


**Figure 5.** Concentration dependent DNA cleavage by  $[V(maltol)_2(dpq)]^+$  (3); [complex] = 100–600  $\mu$ M, [DNA] = 300 ng, incubation time = 40 min, TBE buffer, pH 8.2, 37  $^{\circ}$ C. Gel image (inset) showing the formation of nicked (upper band) and linear (middle band) forms of DNA produced from supercoiled (lower band) DNA as monitored by 1% agarose gel electrophoresis. All lanes contained 300 ng DNA. Lane 1: DNA control, lanes 2–7: 100, 200, 300, 400, 500, and 600  $\mu$ M of 3.

DNA in presence of hydroxyl radical scavengers (DMSO and mannitol), singlet oxygen scavengers (DABCO,  $NaN_3$  and L-histidine), and a superoxide scavenger (superoxide dismutase, SOD) (Figure 6). Partial inhibition of DNA cleavage was observed in presence of DABCO,  $NaN_3$  (lanes 5 and 6 for the dpq complex), and L-histidine (lanes 12, 13, and 14 for the dppz complex). This result indicates that probably singlet oxygen ( $^1O_2$ ) is involved in the DNA cleavage by these complexes. Inhibition of DNA cleavage by SOD was not observed (lanes 8 and 15); instead it was found to be enhanced. Since SOD catalyzes the conversion of free superoxide to hydrogen peroxide, it is thought that this hydrogen peroxide produced is responsible for additional cleavage by 3 and 4.<sup>59</sup> The data indicate that DNA cleavage by 3 and 4 in the absence of any external additives does not proceed via either hydroxyl or superoxide radicals.

**In Vitro Insulin Mimetic Activity.** The insulin mimetic activity of the complexes was estimated by measuring their effect on utilization of glucose in vitro in RIN 5f cell lines. The RIN 5f cell line is a glucose responsive cell line which utilizes the glucose in presence of insulin. The

(59) Han, Y.; Shen, T.; Jiang, W.; Xia, Q.; Liu, C. J. *Inorg. Biochem.* **2007**, *101*, 214.

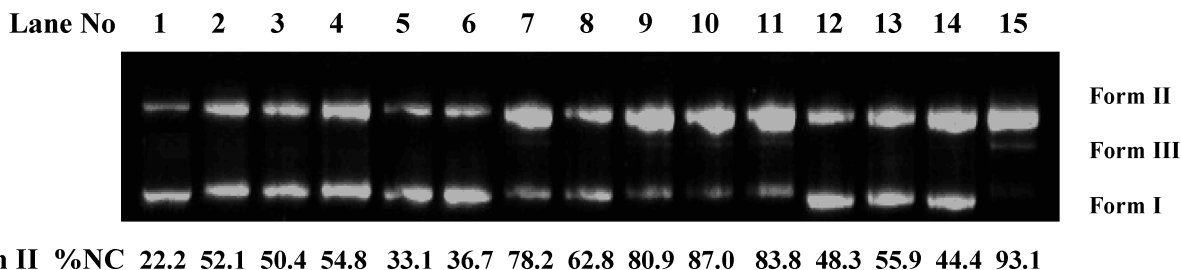


**Figure 6.** Cleavage of plasmid pBR322 DNA (300 ng) in presence of 300  $\mu$ M complexes and different inhibitors after 40 min incubation at 37  $^{\circ}$ C. Lane 1: DNA control, lane 2: DNA + 3, lane 3–8: DNA + 3 + DMSO (1 mM)/manitol (50 mM)/DABCO (10 mM)/NaN<sub>3</sub> (20 mM)/ L-histidine (20 mM)/SOD (15 units), lane 9: DNA + 4, lane 10–15: DNA + 4 + DMSO (1 mM)/manitol (50 mM)/DABCO (10 mM)/NaN<sub>3</sub> (20 mM)/ L-histidine (20 mM)/SOD (15 units).

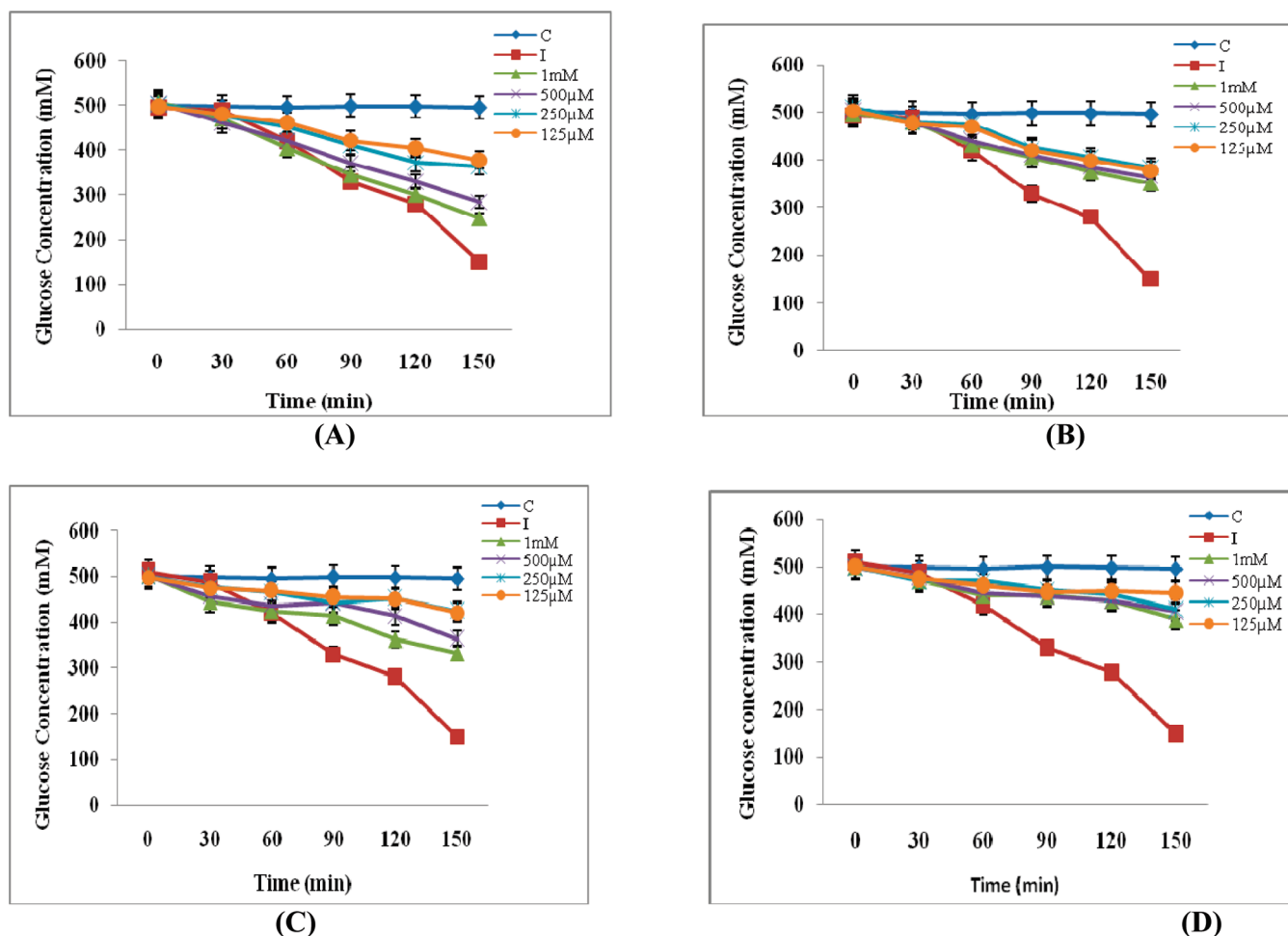


**Figure 7.** Insulin secretion by RIN 5f cells in response to 500 mM glucose in presence of vanadium complexes: (A) complex 1, (B) complex 2, (C) complex 3, and (D) complex 4 with the concentrations 125  $\mu$ M–1 mM. The human recombinant insulin is used as control. Secretion by RIN 5f cells in response to glucose is measured by the DNSA method after every 30 min. The data are indicated as mean  $\pm$  SEM ( $n = 3$ ), and statistical differences (ANOVA) are applied between the control insulin and complexes treated where  $P < 0.05$ .

calculated amount of glucose (500 mM) and different concentrations of vanadium complexes were added and residual glucose was calculated after different time intervals using the DNSA method. Experiments using the RIN 5f cell line show that vanadium complexes (1–4) stimulated glucose utilization in a dose dependent manner over the concentration range 125  $\mu$ M to 1 mM. The maximal insulin response can be compared with the approximate glucose utilization in the cell line induced by vanadium complexes. All the vanadium complexes showed insulin mimetic activity with reduction of the glucose concentration (Figure 7). Complex 1 showed maximum insulin

mimetic activity comparable to pure insulin with 1 mM concentration where the glucose was reduced to 248 mM after 150 min. There is a constant and gradual decrease in glucose concentration with complex 1 per time interval. Complex 3 also shows better mimetic activity with 1 mM concentration in 120 min, whereas the other complexes 2 and 4 show negligible activity with RIN 5f cells. In vitro insulin mimetic activity against insulin responsive RIN 5f cells indicates that complex 1 has a similar activity to insulin while the others have moderate insulin mimetic activity. The mechanisms invoked in the activity of vanadium complexes are the inhibition of protein tyrosine

phosphatases and activation of non-receptor protein tyrosine kinases as well as inhibition of  $\text{Ca}^{2+}$ -ATPase.<sup>60</sup> The studies to identify the mechanisms of these complexes are in progress in our laboratory.

### Conclusion

Vanadium(III) complexes of maltolate and diimine bases have been synthesized and structurally characterized. To our knowledge, this is the first report on the DNA cleavage activity by mononuclear V(III) complexes. We have shown that V(III) complexes of dpq (**3**) and dppz (**4**) ligands are more active than bpy (**1**) and phen (**2**) complexes in cleaving plasmid DNA which also do not require any external reagents like ascorbate or hydrogen peroxide. These reactions appear not to involve either diffusible hydroxyl radicals or free superoxide radicals and are thus different from Fenton type chemistry seen with V(III) monomers in presence of  $\text{H}_2\text{O}_2$ . The possibility of a hydrolytic cleavage mechanism cannot be ruled out. Further work to elucidate the mechanism

is presently underway in our laboratory. The complexes show in vitro insulin mimetic activity against insulin responsive RIN 5f cells, with complex **1** being the most potent which is comparable to insulin at the complex concentration of 1 mM, while the others have moderate insulin mimetic activity.

**Acknowledgment.** M.N.I. acknowledges the Indian Council for Cultural Relations (ICCR), New Delhi, India, for financial support. A.A.K. acknowledges funding from University of Pune. A.S.K. acknowledges funding from DST, New Delhi, (SR/S5/BC-25/2006), UGC, New Delhi (F. No. 32-198/2006(SR)) and University of Pune for partial funding. The authors thank Mr. Satish Bhat for growing crystals of complexes. The X-ray diffractometer at YSU was funded by NSF Grant 0087210, Ohio Board of Regents Grant CAP-491, and by Youngstown State University.

**Supporting Information Available:** Complete ORTEP diagrams of complex **1**, **2**, and **3** (Figure S1, S2, and S3). The packing diagrams of complex **1**, **2**, and **3** (Figure S4, S5, S6), the cyclic voltammogram of complexes **2–4** (Figure 7–S9), and the Spectro-electrochemistry of the **2–4** (Figure S10–S12). This material is available free of charge via the Internet at <http://pubs.acs.org>. CCDC 742059 (Complex **1**), CCDC 742060 (Complex **2**), and CCDC 785387 (Complex **3**) contain the supplementary crystallographic data and can be obtained free of charge via [www.ccdc.cam.ac.uk/conts/retrieving.html](http://www.ccdc.cam.ac.uk/conts/retrieving.html) (or from the Cambridge Crystallographic Data Centre, 12 Union Road, Cambridge CB2 1EZ, U.K.; fax: (+44)1223-336-033; or deposit@ccdc.cam.ac.uk).

(60) (a) *Bioinorganic Vanadium Chemistry*; Rehder, D., Ed.; John Wiley & Sons, Ltd: West Sussex, England, 2008. (b) Thompson, K. H.; Lichter, J.; LeBel, C.; Scaife, M. C.; McNeill, J. H.; Orvig, C. *J. Inorg. Biochem.* **2009**, *103*, 554. (c) Smee, J. J.; Epps, J. A.; Ooms, K.; Bolte, S. E.; Polenova, T.; Baruah, B.; Yang, L.; Ding, W.; Li, M.; Willsky, G. R.; Cour, A. I.; Anderson, O. P.; Crans, D. C. *J. Inorg. Biochem.* **2009**, *103*, 575. (d) Li, M.; Ding, W.; Baruah, B.; Crans, D. C.; Wang, R. *J. Inorg. Biochem.* **2008**, *102*, 1846. (e) Aureliano, M.; Henao, F.; Tiago, T.; Duarte, R. O.; Moura, J. J. G.; Baruah, B.; Crans, D. C. *Inorg. Chem.* **2008**, *47*, 5677.